PHYSICAL REVIEW B VOLUME 30, NUMBER 4 15 AUGUST 1984

Absorption spectrum of clusters of spheres from the general solution of Maxwell's equations. III. Heterogeneous spheres

J. M. Gérardy*
Institut Montefiore B28, Université de Liège, B-4000 Liège, Belgium

M. Ausloos†
Institut de Physique B5, Université de Liège, B-4000 Liège, Belgium

(Received 10 November 1983)

We present the solution of Maxwell's equations for an arbitrary distribution of heterogeneous spheres taking into account cluster geometry, retardation effects, all multipolar (electric and magnetic) order interactions, and any arbitrary light incidence. The fields are expanded in terms of the usual spherical wave-vector functions. Usual boundary conditions are applied at each interface. The problem consists in obtaining the appropriate microscopic effective susceptibility for the heterogeneous spheres, and the appropriate rewriting of the interaction and field terms. In so doing the solution of the problem is similar to that for homogeneous spheres [Phys. Rev. B 25, 4204 (1982)]. We specialize the boundary-condition problem to the case of a metallic nucleus containing plasmons and of a dielectric shell. Simpler cases are also examined: the plasmonless limit, the single sphere, the hollow sphere, and the long-wavelength limit. Numerical results are presented to show various parameter effects; the field expansions are limited to, but inlcude, the octupolar terms.

I. INTRODUCTION

In a previous paper, hereafter referred to as I, we have presented a theory of infrared- (ir-) absorption spectrum of (ionic) powders through the solution of Maxwell's equations up to a given 2^l polar order in the long-wavelength limit.[1] At topical conferences, we have illustrated the results and discussed effects due to quadrupolar and octupolar field distributions in the particles.[2-4] In all cases the particles are supposed to be spheres, but spheroids can be easily treated in the same framework. Although removal of the long-wavelength approximation and of restrictions on the assumed spherical shape of the particles, as well as the neglect of retardation effects, would have likely improved the theoretical description of the experimental data on ionic powders, we have preferred, when rewriting the general theory, to apply it to metallic inclusions in some matrix.[5]

Therefore, in paper II of this series,[5] we have examined the optical properties of spherical "metallic" particles. We have taken into account finite-wavelength effects, a plasmon-dependent dielectric function, retardation effects, and multipolar interactions between particles in contact or not. In so doing we have in fact generalized Ruppin's theory[6] for isolated metallic particles. Notice that the percolation transition was not part of such a theory.

Next we want to treat more realistic cases. It is apparent from published work (in particular from various papers found in conference proceedings[7-10]) that *homogeneous* particles are exceptions rather than rules, due to particle production processes. Therefore, in this paper (III) we intend to describe the infrared absorption and related properties of heterogeneous particles. The model in mind is that of concentric shells.

We admit that much theoretical and experimental work has already been presented in the literature on the subject. On homogeneous (metallic) particles, a recent review article by Perenboom *et al.* is available.[11] No complete review of work on heterogeneous particles is attemped here, but one can recall that the first applications of Mie theory to the scattering of electromagnetic waves by (two) concentric spheres are due to Güttler[12] and Aden and Kerker.[13] The latter work was expanded by Kerker[14] and various collaborators in order to describe many different aspects of concentric (or confocal) particles.[14,15] In the same framework, let us mention work by Bohren,[16] Gordon and Holzwarth,[17] and Latimer and Wamble.[18] The first work deals with a spherical shell having an anisotropic index of refraction, while the third considers particles of a dimension that is larger than the wavelength of light, and in particular hollow spheres. In addition to such work related to the description of aggregation processes of colloids, let us mention another nested model of layered spheres (for phosphorus-derived smoke) by Milham *et al.*[19] and in the same spirit by Blum and Frisch.[20]

Another ensemble of papers[21-23] is more related to work on percolation aspects than on colloidal aggregation, and therefore has considered to a greater degree surface effects as well as effects due to the inner *metallic core* as opposed to those due to a polymeric shell. Nevertheless, in Refs. 21–23, in the first theoretical attempts is a discussion of the positions of plasma resonances in particles containing a *dielectric* seed or *nucleus,*[21] following observations by Genzel *et al.*[22] This was followed by a detailed calculation of the optical-absorption coefficients of metallic shells on dielectric cores by Granqvist and Hunderi.[23]

The optical properties of fine metallic particles covered by an oxide, sulfide, etc., pellicle were discussed by Granqvist *et al.*,[24] following other observation of surface modes in oxide-coated metal spheres by Martin,[25] and their prediction by Ruppin,[26] on isolated particles. In the same line of investigations let us recall an "intermediary case:" that of small silicon particles with oxide overlayers.[27] Such work intended to obtain an effective dielectric constant through a description of the polarizability of the particle. Since a Maxwell-Garnett description was attempted, the particles were supposed to be randomly distributed in the matrix.

Independently, Clippe *et al.*[28–30] were the first to recognize the importance of short-range order and of particular clusters in describing optical properties of aggregates. Their theory based on a simple dipole-dipole coupling (between homogeneous spheres) had shortcomings already discussed elsewhere.[1] Nevertheless, such recognition and its experimental interest[24,31] motivates work in the area bounded by the "isolated particle" on one hand and the "random medium" cases on the other hand. Hence our theory attempts to fill this gap.[32] We wish to conclude this review by mentioning other related work on the effective-medium theory of optical properties of small heterogeneous particle composites.[33,34]

Nevertheless, we want to stress that our main goal is to describe the functional dependence of the observed (or observable) light on the state of aggregation of heterogeneous particles irrespective of percolation phenomena. Furthermore, we do not look for criteria allowing one to select appropriate aggregation or aggregate models, but we hope to present a (useful) theory from which such criteria might be derived, and thereby answer a complaint, e.g., in Ref. 18, that "for real random aggregates, the direct solution of Maxwell's equations is impractical." Our theoretical results are in a form which can be used on a computer, as we will demonstrate, and are available for more complex problems or more general systems.

In Sec. II we explicitly give the full theory generalizing that of Ref. 5, at the level of more complicated boundary conditions, i.e., supposing that plasmons exist in one of the materials (here taken to be the nucleus). In Sec. III we consider the plasmonless case. In Sec. IV we show that we recover the isolated spherical particle case from our general expressions; we also consider the hollow sphere. In Sec. V we take the long-wavelength approximation for the main results of Sec. II and recover well-known expressions. In Sec. VI we particularize our results to a simple case in order to present numerical results; in so doing, we can discuss various effects, in particular, that of multipole-multipole interactions. In an appendix, we consider the case in which the nucleus is a dielectric and the layer is metallic, in order to be able to use an analogy for understanding the qualitative properties of clusters containing such a type of particle.

II. THEORY

Our theory follows that of Ref. 5. We strongly reduce the generality of our investigation from the beginning. However, in the line of our previous work[1–5] it is clear that several assumptions can be removed, but one must then resort to much more complicated algebra and notation. We expect that our results may be of general interest, however, and hope that they suggest areas of further investigation.

We consider a *simple* geometry for the heterogeneous particles. They are supposed to be made of two concentric spheres. The inner material is called the nucleus (N); it is surrounded by a shell (S). The nucleus radius is called R_N. The nucleus and the shell materials are characterized by their respective dielectric function $\epsilon(\vec{k},\omega)$ and magnetic permeability $\mu(\omega)$. We wish in the main theoretical section to take into account the possibility of plasmon excitations, and to consider a very general form of $\epsilon(\vec{k},\omega)$ as long as N and S have a metallic character in the bulk limit. Therefore, we introduce the notations ϵ_N^T, ϵ_S^T, ϵ_N^L, ϵ_S^L, μ_N, and μ_S, where L and T refer to the longitudinal and transverse part, respectively, of the propagating wave in the particle. The matrix characteristic functions are supposed to be frequency independent; they are called ϵ_M and μ_M.

Several combinations of N and S materials can be envisaged. A metallic particle can be grown from an insulatorlike nucleus, or a metallic particle can be coated by its oxide, by a nitrite layer, or by a totally different material (such as a dye). The layer-coated metal particles seem to be of interest. One "restriction" is thus made at this point: Only the nucleus has metallic character. Therefore, we assume that there is no plasmon in the shell. Such restrictions can be removed when appropriate experimental work has to be analyzed. From examples treated in Refs. 1–5 and our unpublished work, it appears that the distinction between metallic or dielectric spheres is only of quantitative nature when discussing the mode positions and the overall shape of an ir-absorption spectrum. The above restriction on the character of N or S thus has a mild importance.

The solution of the electromagnetic problem (Laplace's equation) consists of obtaining the correct coefficients for the field expansions in the various media by applying appropriate boundary conditions. (We avoid writing the time dependence $e^{i\omega t}$ in the following.) Let the electric field in the shell of particle B be given by

$$\vec{E}_B^S = E \sum_{p,q} (a_{p,q}^S \vec{m}_{pq1} + b_{p,q}^S \vec{n}_{pq1} + e_{p,q}^S \vec{l}_{pq1} + c_{p,q}^S \vec{m}_{pq3} + d_{p,q}^S \vec{n}_{pq3} + f_{p,q}^S \vec{l}_{pq3}) , \tag{1}$$

where the $\vec{m}_{pq}$, $\vec{n}_{pq}$, and $\vec{l}_{pq}$ functions are the spherical wave-vector functions defined in Ref. 5; the indices 1 and 3 indicate, respectively, the Bessel $j_q(x)$ or Neumann $h_q^{(1)}(x)$ function. We have not indicated in Eq. (1), nor in the following, the variable $\vec{r}$ in the functions as long as there is no confusion. The magnetic field is similarly expanded,

$$\vec{H}_B^S = \frac{c k_S^T E}{i\omega\mu_S} \sum_{p,q} (b_{p,q}^S \vec{m}_{pq1} + a_{p,q}^S \vec{n}_{pq1} + d_{p,q}^S \vec{m}_{pq3} + c_{p,q}^S \vec{n}_{pq3}) , \tag{2}$$

where c is the speed of light.

We do not consider the case where longitudinal magnons would be present, that is why the $\vec{l}_{pq}$ function does not appear in Eq. (2). The electric and magnetic fields in the nucleus ($\vec{\mathrm{E}}_B^N$ and $\vec{\mathrm{H}}_B^N$) are given by, respectively,

$$\vec{\mathrm{E}}_B^N=E\sum_{p,q}(a_{p,q}^N\vec{\mathrm{m}}_{pq\,1}+b_{p,q}^N\vec{\mathrm{n}}_{pq\,1}+e_{p,q}^N\,\vec{\mathrm{l}}_{pq\,1}) \tag{3}$$

and

$$\vec{\mathrm{H}}_B^N=\frac{ck_N^TE}{i\omega\mu_N}\sum_{p,q}(b_{p,q}^N\vec{\mathrm{m}}_{pq\,1}+a_{p,q}^N\vec{\mathrm{n}}_{pq\,1}) \ . \tag{4}$$

These fields cannot be expanded in terms of the $\vec{\mathrm{m}}_{pq\,3}$, $\vec{\mathrm{n}}_{pq\,3}$, and $\vec{\mathrm{l}}_{pq\,3}$ functions because of the smooth behavior prevalent at the center of the sphere.

The external field (due to the scattering on the jth sphere) is expanded accordingly in the matrix,

$$\vec{\mathrm{E}}_M^{(j)}=E\sum_{p,q}^{(j)}(c_{p,q}^M\vec{\mathrm{m}}_{pq\,3}+d_{p,q}^M\vec{\mathrm{n}}_{pq\,3}) \ , \tag{5}$$

$$\vec{\mathrm{H}}_M^{(j)}=\frac{ckE}{i\omega\mu_M}\sum_{p,q}^{(j)}(d_{p,q}^M\vec{\mathrm{m}}_{pq\,3}+c_{p,q}^M\vec{\mathrm{n}}_{pq\,3}) \ , \tag{6}$$

where k_S^T, k_N^T, and k is the wave number in the shell, nucleus, and matrix, respectively. For transverse waves it is given by the solution of the dispersion relation,

$$k^2c^2=\omega^2\epsilon^T(\vec{\mathrm{k}},\omega)\mu(\omega) \ , \tag{7}$$

with the appropriate ϵ^T function. On the other hand, longitudinal waves can propagate in the nucleus if

$$\epsilon_N^L(\vec{\mathrm{k}},\omega)=0 \ . \tag{8}$$

Solutions of Eqs. (7) and (8) are chosen such that $\vec{\mathrm{k}}$ has a positive imaginary part.

The coefficients $d_{p,q}^M$ and $c_{p,q}^M$, as well as the functions $\vec{\mathrm{n}}_{pq\,3}$ and $\vec{\mathrm{m}}_{pq\,3}$ in Eqs. (5) and (6), are supposed to be defined in the j frame centered on the jth sphere. The total field in the matrix is a linear superposition of the total scattered ($\vec{\mathrm{E}}_M^{(j)},\vec{\mathrm{H}}_M^{(j)}$) field and of the externally applied field defined by

$$\vec{\mathrm{E}}_0=E_0\sum_{p,q}^{(i)}(a_{p,q}^I\vec{\mathrm{m}}_{pq\,1}+b_{p,q}^I\vec{\mathrm{n}}_{pq\,1}) \ , \tag{9}$$

$$\vec{\mathrm{H}}_0=H_0\sum_{p,q}^{(i)}(b_{p,q}^I\vec{\mathrm{m}}_{pq\,1}+a_{p,q}^I\vec{\mathrm{n}}_{pq\,1}) \ , \tag{10}$$

where we recall that the coefficients and variables depend on the reference (i) frame. In doing such a summation any retardation effect is automatically taken into account.

A. Nucleus-shell boundary problem

The boundary conditions (BC's) have been recalled by Ruppin following a discussion on the correct set of BC's for a conducting medium by Melnyk and Harrison.[35] The BC's are the continuity of tangential $\vec{\mathrm{E}}$ and $\vec{\mathrm{H}}$ and normal displacement current, the condition on the normal magnetic-flux density being superfluous. Hence at the *inner* interface, one requires

$$\vec{\mathrm{E}}_B^S\times\vec{\mathrm{l}}_{R_N}=\vec{\mathrm{E}}_B^N\times\vec{\mathrm{l}}_{R_N} \ , \tag{11a}$$

$$\vec{\mathrm{H}}_B^S\times\vec{\mathrm{l}}_{R_N}=\vec{\mathrm{H}}_B^N\times\vec{\mathrm{l}}_{R_N} \ , \tag{11b}$$

$$\epsilon_S\vec{\mathrm{E}}_B^S\cdot\vec{\mathrm{l}}_{R_N}=\epsilon_N\vec{\mathrm{E}}_B^N\cdot\vec{\mathrm{l}}_{R_N} \ . \tag{11c}$$

The first two conditions lead, after some algebra, to four equations involving the defining coefficients $a_{p,q}^S,\ldots,c_{p,q}^N$ of Eqs. (1)–(4). Each equation can be separated into two relations according to the angular dependence. Equation (11a) leads to

$$a_{p,q}^Sj_q(x_S)+c_{p,q}^Sh_q^{(1)}(x_S)=a_{p,q}^Nj_q(x_N) \ , \tag{12}$$

$$\begin{aligned}b_{p,q}^S\frac{1}{x_S}\left[\frac{d}{dx}xj_q(x)\right]_{x_S}+d_{p,q}^S\frac{1}{x_S}\left[\frac{d}{dx}xh_q^{(1)}(x)\right]_{x_S}\\=b_{p,q}^N\frac{1}{x_N}\left[\frac{d}{dx}xh^{(1)}(x)\right]_{x_N}+e_{p,q}^N\frac{1}{x_N}j_q(y_N) \ ,\end{aligned} \tag{13}$$

where

$$x_S=k_S^TR_N \ , \tag{14}$$

$$x_N=k_N^TR_N \ , \tag{15}$$

$$y_N=k_N^LR_N \ . \tag{16}$$

Equation (11b) similarly leads to

$$\frac{x_S}{\mu_S}[b_{p,q}^Sj_q(x_S)+d_{p,q}^Sh_q^{(1)}(x_S)]=\frac{x_N}{\mu_N}b_{p,q}^Nj_q(x_N) \ , \tag{17}$$

$$\begin{aligned}\frac{1}{\mu_S}\left[a_{p,q}^S\left[\frac{d}{dx}xj_q(x)\right]_{x_S}+c_{p,q}^S\left[\frac{d}{dx}xh_q^{(1)}(x)\right]_{x_s}\right]\\=\frac{1}{\mu_N}a_{p,q}^N\left[\frac{d}{dx}xj_q(x)\right]_{x_N} \ .\end{aligned} \tag{18}$$

The third BC, (11c), leads to

$$\begin{aligned}b_{p,q}^Sq(q+1)j_q(x_S)/x_S+d_{p,q}^Sq(q+1)h_q^{(1)}(x_S)/x_S\\=b_{p,q}^Nq(q+1)j_q(x_N)/x_N+e_{p,q}^Nk_N^L\left[\frac{d}{dy}j_q(y)\right]_{y_N} \ .\end{aligned} \tag{19}$$

From (12) and (18) one can obtain $a_{p,q}^S$ and $c_{p,q}^S$ as a function of $a_{p,q}^N$ in terms of proportionality coefficients which can be called "2^q polar-interface susceptibilities," i.e.,

$$a_{p,q}^S=\Gamma_q^{(1)}a_{p,q}^N \ , \tag{20a}$$

$$c_{p,q}^S=\Gamma_q^{(2)}a_{p,q}^N \ , \tag{20b}$$

with

$$\Gamma_q^{(1)}=\left[\frac{h_q^{(1)}(x_N)}{j_q(x_S)}\right]\left[\frac{h_q^{(1)+}(x_S)-(\mu_S/\mu_N)j_q^+(x_N)}{h_q^{(1)+}(x_S)-j_q^+(x_S)}\right] \tag{21a}$$

and

$$\Gamma_q^{(2)}=\left[\frac{j_q(x_N)}{h_q^{(1)}(x_S)}\right]\left[\frac{(\mu_S/\mu_N)j_q^+(x_N)-j_q^+(x_S)}{h_q^{(1)+}(x_S)-j_q^+(x_S)}\right] \ , \tag{21b}$$

where any $g^+(z)$ function is defined by

$$g^+(z)=\frac{1}{g(z)}\frac{d}{dz}zg(z)\ . \tag{22}$$

Notice that these $\Gamma_q^{(i)}$ functions are "mere" generalizations of that Γ_q found in Ref. 5 [Eq. (12d) in the case of a metal-particle—matrix interface]. Notice also that Eqs. (20a) and (20b) are mere proportionality relations and do not involve convolutions.

We still must obtain $b_{p,q}^S$ and $d_{p,q}^S$ from the other equations. After some algebra one finds

$$b_{p,q}^S=\Delta_q^{(1)}b_{p,q}^N\ , \tag{23a}$$

$$d_{p,q}^S=\Delta_q^{(2)}b_{p,q}^N\ , \tag{23b}$$

where

$$\Delta_q^{(1)}=\left[\frac{k_S^T j_q(x_N)}{k_N^T j_q(x_S)}\right]\left[\frac{(\epsilon_N^T/\epsilon_S)[j_q^+(x_S)-f_q(y_N)]-j_q^+(x_N)+f_q(y_N)}{(\epsilon_N^T/\epsilon_S)[h_q^{(1)+}(x_S)-f_q(y_N)]-j_q^+(x_S)+f_q(y_N)}\right]\ , \tag{24a}$$

$$\Delta_q^{(2)}=\left[\frac{k_S^T j_q(x_N)}{k_N^T h_q^{(1)}(x_S)}\right]\left[\frac{(\epsilon_N^T/\epsilon_S)[j_q^+(x_S)-f_q(y_N)]-j_q^+(x_N)+f_q(y_N)}{(\epsilon_N^T/\epsilon_S)[h_q^{(1)+}(x_S)-f_q(y_N)]-j_q^+(x_S)+f_q(y_N)}\right]\ , \tag{24b}$$

where

$$f_q(y_N)\equiv q(q+1)j_q(y_N)\Big/\left[y\frac{d}{dy}j_q(y)\right]_{y_N}\ . \tag{25}$$

Here, we do not write $c_{p,q}^S$ in terms of $b_{p,q}^N$, but it could be obtained by combining Eqs. (23) and (24) with Eq. (13). On the other hand, notice that y_N (related to longitudinal plasmons) does not appear in the "magnetic" susceptibilities $\Delta_q^{(i)}$.

B. Shell-matrix boundary problem and solution for the external coefficients

The description of the scattered field by an ensemble of heterogeneous spheres interacting with each other follows the method described in Ref. 5 step by step (Sec. II B). The idea is to express the mutual interactions of particles by a projection technique in order to obtain matrix elements for interaction terms. Then writing the BC at the shell-matrix interface, one is led to a set of linear equations between the coefficients of the applied field expansions and those of the scattered fields. The main difference with respect to the system of equations (22) found in Ref. 5 consists in the formal expression for the scattered field coefficients which take into account, here, the heterogeneous nature of particles. Therefore, here we only give the appropriate modifications, i.e., those defining the unknown vectors $\vec{c}^{\,M}$ and $\vec{d}^{\,M}$ in terms of $\vec{a}^{\,I}$ and $\vec{b}^{\,I}$.

For example, the corresponding set of equations relating the field coefficients in the matrix to those in (on) the shell is found from the BC on the electric field to be

$$\sum_{j\neq i}^{N}\sum_{p,q}\{[c_{p,q}^M(j)\langle M\mid M\rangle_i+d_{p,q}^M(j)\langle N\mid M\rangle_i]h_q^{(1)}(x_i)+e^{iz_i}a_{l,m}^I j_m(x_i)\}=a_{l,m}^N(i)j_m(\bar{x}_{Si})C_m(i)\ , \tag{26}$$

$$\sum_{j\neq i}^{N}\sum_{p,q}\{[c_{p,q}^M(j)\langle M\mid N\rangle_i+d_{p,q}^M(j)\langle N\mid N\rangle_i]h_q^{(1)}(x_i)+e^{iz_i}b_{l,m}^I j_m(x_i)[j_m^+(x_i)/h_m^{(1)+}(x_i)]\}$$
$$=b_{l,m}^N(i)(x_i/\bar{x}_{Si})j_m(\bar{x}_{Si})[j_m^+(\bar{x}_{Si})/h_m^{(1)+}(x_i)]D_m(i)\ , \tag{27}$$

where in order to simplify the writing, we have already used (23) for expressing the right-hand side of Eqs. (26) and (27). In so doing we have directly related the "matrix coefficients" to the "nucleus coefficients." Nevertheless, some word on the notations is necessary. We have used a notation such as $\langle M\mid N\rangle_i$ such that

$$\langle M\mid N\rangle_i\equiv\langle\vec{m}_{pq3}(j)\mid\vec{n}_{lm3}(i)\rangle\ , \tag{28}$$

with the usual definition of the brackets $\langle\cdots\mid\cdots\rangle$ [Eq. (17) in Ref. 5]. Such notation is unambiguous with respect to the indices indeed because of the orthogonality and completeness relations given by Stratton as discussed in Ref. 5. Furthermore,

$$x_i\equiv kR_i \tag{29}$$

and

$$\bar{x}_{Si} \equiv k_S^T R_i \ , \tag{30}$$

where R_i is the *total* radius of sphere i, and k (k_S^T) is as before the wave vector in the matrix (shell).

In order to calculate matrix elements no particular reference frame has to be singled out. However, the overall geometry must be defined in order to be able to define the "external field." Therefore, the origin of axes must be chosen. It seems natural to refer to some particular sphere 0 in the sample as being at the origin of axes. Another sphere, for instance, i, will, according to theory, be located at (r_1, r_2, r_3). One defines

$$z_i \equiv k r_3 \ . \tag{31}$$

Furthermore, the incident field phase is supposed to be zero at the center of the 0 sphere. Therefore, we let $a_{p,q}^I \equiv a_{p,q}^I(0)$ and $b_{p,q}^I \equiv b_{p,q}^I(0)$. Finally,

$$C_q = \frac{j_q(x_N)}{h_q^{(1)+}(x_N) - j_q(x_N)} \left[\frac{h_q^{(1)+}(x_S)}{j_q(x_S)} - r_q(\bar{x}_S) \frac{j_q^+(x_S)}{h_q(x_S)} - \frac{\mu_S}{\mu_N} j_q^+(x_N) \left[\frac{1}{j_q(x_S)} - r_q(\bar{x}_S) \frac{1}{h_q^{(1)}(x_S)} \right] \right] , \tag{32}$$

$$\begin{aligned} D_q = \frac{x_S}{x_N} \frac{j_q(x_N)}{h_q^{(1)+}(x_S) - j_q^+(x_S)} & \left[\frac{\epsilon_N}{\epsilon_S} \left[\frac{h_q^{(1)+}(x_S)}{j_q(x_S)} - s_q(\bar{x}_S) \frac{j_q^+(x_S)}{h_q^{(1)+}(x_S)} \right] \right. \\ & \left. - \left[1 - \frac{\epsilon_N}{\epsilon_S} \right] [j_q^+(x_N) - f_q(y_N)] \left[\frac{1}{j_q(x_S)} - s_q(\bar{x}_S) \frac{1}{h_q^{(1)}(x_S)} \right] \right] , \end{aligned} \tag{33}$$

in which the index of sphere i has been omitted, and where we have introduced the functions

$$r_q(z) = h_q^{(1)}(z) / j_q(z) \tag{34}$$

and

$$s_q(z) = r_q(z) h_q^{(1)+}(z) / j_q^+(z) \ . \tag{35}$$

Similarly, the magnetic BC leads to a set of equations which after some algebra reduces to

$$\sum_{\substack{j=1 \\ j \neq i}}^{N} \sum_{p,q} [c_{p,q}^M(j) \langle M \mid M \rangle_i + d_{p,q}^M(j) \langle N \mid M \rangle_i] h_q^{(1)}(x_i) + e^{iz_i} b_{l,m}^I j_m(x_i) = b_{l,m}^N(i) j_m(\bar{x}_{Si}) (\mu_M / \mu_S)(\bar{x}_{Si} / x_i) E_m(i) \ , \tag{36}$$

$$\begin{aligned} \sum_{\substack{j=1 \\ j \neq i}}^{N} \sum_{p,q} [c_{p,q}^M(j) \langle M \mid N \rangle_i + d_{p,q}^M(j) \langle N \mid N \rangle_i] h_q^{(1)}(x_i) + e^{iz_i} a_{l,m}^I j_m(x_i) [j_m^+(x_i) / h_m^{(1)+}(x_i)] & \\ = a_{l,m}^N(i) (\mu_M / \mu_S) j_m(\bar{x}_{Si}) [j_m^+(\bar{x}_{Si}) / h_m^{(1)+}(x_i)] F_m(i) \ . & \end{aligned} \tag{37}$$

The definitions for $E_m(i)$ and $F_m(i)$ are given in short by the following correspondence laws:

$$E_m(i) \equiv D_m(i) \quad \text{where } s_m(\bar{x}_S) \rightarrow r_m(\bar{x}_S) \tag{38}$$

and

$$F_m(i) \equiv C_m(i) \quad \text{where } r_m(\bar{x}_S) \rightarrow s_m(\bar{x}_S) \ . \tag{39}$$

The system (26), (27), (36), and (37) can be solved for the exterior (matrix) coefficients in terms of the external field coefficients by eliminating those describing the nucleus. It may be of interest to write such a solution under a rather compact form. On one hand, this allows a better visual comparison with the system of Eqs. (20) and (21) of Ref. 5. One has, after some algebra,

$$\begin{aligned} \sum_{\substack{j=1 \\ j \neq i}}^{N} \sum_{p,q} \{ c_{p,q}^M(j) [\sigma_m(i) \langle N \mid N \rangle_i - \tau_m(i) \langle M \mid M \rangle_i] + d_{p,q}^M(j) [\sigma_m(i) \langle M \mid N \rangle_i - \tau_m(i) \langle N \mid M \rangle_i] \} & \\ = e^{iz} a_{l,m}^I T_m(i) j_m(x_i) / h_m^{(1)}(x_i) \ , & \end{aligned} \tag{40}$$

$$\begin{aligned} \sum_{\substack{j=1 \\ j \neq i}}^{N} \sum_{p,q} \{ d_{p,q}^M(j) [\rho_m(i) \langle M \mid N \rangle_i - \kappa_m(i) \langle N \mid M \rangle_i] + c_{p,q}^M(j) [\rho_m(i) \langle N \mid N \rangle_i - \kappa_m(i) \langle M \mid M \rangle_i] \} & \\ = e^{iz} b_{l,m}^I K_m(i) j_m(x_i) / h_m^{(1)}(x_i) \ , & \end{aligned} \tag{41}$$

where (omitting the reference to the sphere label)

$$\sigma_q = (\mu_s/\mu_M) h_q^{(1)+}(x) \ , \tag{42a}$$

$$\tau_q = (F_q/C_q) j_q^{+}(\bar{x}_S) \ , \tag{42b}$$

$$\rho_q = -(\mu_M/\mu_S)\sigma_q \ , \tag{42c}$$

$$\kappa_q = -(\epsilon_M/\epsilon_S^T)(D_q/E_q) j_q^{+}(\bar{x}_S) \ , \tag{42d}$$

and

$$T_q = \tau_q - (\mu_S/\mu_M) j_q^{+}(x) \ , \tag{42e}$$

$$K_q = \kappa_q + j_q^{+}(x) \ . \tag{42f}$$

It is then clear that only a numerical solution can be pursued after precising a cluster geometry and calculating the interaction matrix elements. In principle, such terms can be obtained analytically. We have given all the necessary information for calculating them up to the $l = p = 4$ in Ref. 5.

III. PLASMONLESS CASE

In this paper we do not write the above system of equations when the nucleus is a dielectric and the shell has a metalliclike character. However, it is of interest to consider an "intermediary" case in which one can neglect plasmons in the nucleus: either a heterogeneous particle is made of two dielectrics, or the frequency of the radiation field is much below the bulk plasmon frequency ω_p. We have shown in paper II that the absorption spectrum can be divided into two regions, one on each side of ω_p. For the low-frequency region, surface modes exist superimposed on the tail of surface-plasmon resonances (of the bulk material) which peak in the ultraviolet region, far above ω_p. On the other hand, the Ruppin ripples at $\omega > \omega_p$ have almost no influence on the $\omega < \omega_p$ resonances.

From the above derivation, it is easy to see the plasmon influence in the theoretical results. The first remark applies to the writing of the set of relations (20)–(23) between the shell and the nucleus coefficients. It readily appears that the magnetic part of these relations does not contain plasmon effects. The second point to be emphasized is the importance of the function $f_q(z)$. As noted in paper II when there is no (or a few) longitudinal plasmon(s) in the material, this implies a very large value of $\operatorname{Im} k^L$, and hence

$$\lim_{k_L \to \infty} f_q(k_N^L R_N) = -i/(k_N^L R_N) \sim 0 \ . \tag{43}$$

It is therefore extremely easy to rewrite the plasmonless case from the above results. The coefficients D_q, E_q, and hence κ_q have a more simple form which will be found at the end of the next section; they also pertain to the single-particle case.

IV. ISOLATED-SPHERE CASE

A. General case

As can be observed from Eq. (23), internal interface resonances appear where the denominator of the electrical susceptibilities $\Delta_q^{(i)}$ vanishes, i.e., when

$$\epsilon_N^T = \frac{j_q^{+}(x_S) - f_q(y_N)}{h_q^{+}(x_S) - f_q(y_N)} \epsilon_S \ . \tag{44}$$

The resonances due to the particle-matrix interface are, on the other hand, obtained from the determinant of the fundamental set of equations (40) and (41). Inspection or direct calculation leads to the resonance conditions

$$\rho_q(i) = \kappa_q(i) \ , \tag{45}$$

$$\sigma_q(i) = \tau_q(i) \ . \tag{46}$$

The latter equation leads to

$$\epsilon_S = -\frac{D_q h_q^{(1)+}(x)}{E_q j_q^{+}(\bar{x}_S)} \epsilon_M \ . \tag{47}$$

One could similarly obtain the "magnetic resonance" conditions.

Let us note that such formulas generalize the Fröhlich condition $(\epsilon + 2\epsilon_M = 0)$ for the surface-mode resonances and the Van de Hulst effective dielectric constant of a coated sphere,

$$\epsilon_{cS} = \frac{2\epsilon_S + \epsilon_N + 2Q^3(\epsilon_N - \epsilon_S)}{2\epsilon_S + \epsilon_N - Q^3(\epsilon_N - \epsilon_S)} \epsilon_S \ , \tag{48}$$

where

$$Q = 1 - (t/R) = R_N/R \tag{49}$$

if t is the thickness of the shell $(t = R - R_N)$.

B. Plasmonless limit $(\omega \ll \omega_p)$

Let us consider the "most interesting" region, i.e., below ω_p. The following asymptotic expressions are very useful:

$$\begin{aligned} &j_q(z) \sim z^q/(2q+1)!! \ , \\ &h_q^{(1)}(z) \sim -i(2q-1)!!/z^{q+1} \ , \\ &j_q^{+}(z) \sim q+1 \ , \\ &h_q^{(1)+}(z) \sim -q \ . \end{aligned} \tag{50}$$

Hence

$$r_q(z) \sim -i(2q-1)!!(2q+1)!!/z^{2q+1} \ , \tag{51a}$$

$$s_q(z) \sim i(q/q+1)(2q-1)!!(2q+1)!!/z^{2q+1} \ . \tag{51b}$$

Immediately (again omitting the label i for the ith sphere),

$$C_q \sim \frac{1}{2q+1}\left[\frac{k_N}{k_S}\right]^q \times \left\{ q + (q+1)\left[\frac{\mu_S}{\mu_N} + \left[\frac{R_N}{R}\right]^{2q+1}\left[1 - \frac{\mu_S}{\mu_N}\right]\right]\right\} \tag{52}$$

and

$$F_q \sim \frac{1}{2q+1}\left[\frac{k_N}{k_S}\right]^q \times \left\{ q+(q+1)\left[\frac{\mu_S}{\mu_N}-q\left[\frac{R_N}{R}\right]^{2q+1}\left[1-\frac{\mu_S}{\mu_N}\right]\right]\right\} . \tag{53}$$

One observes that $C_q = F_q = 1$ if the sphere is homogeneous ($\mu_N = \mu_S$). For a small shell thickness one has

$$C_q \sim (k_N/k_S)^q , \tag{54a}$$

$$F_q \sim (\mu_S/\mu_N)(k_N/k_S)^q . \tag{54b}$$

Consider next the "electrical coefficients," and a plasmonless nucleus. In the low-frequency limit, one has

$$D_q \sim \frac{1}{2q+1}\left[\frac{k_N}{k_S}\right]^{q-1}\left[(q+1)+q\left[\frac{\epsilon_N^T}{\epsilon_S^T}\right] + q\left[\frac{R_N}{R}\right]^{2q+1}\left[1-\frac{\epsilon_N^T}{\epsilon_S^T}\right]\right] , \tag{55}$$

$$E_q \sim \frac{1}{2q+1}\left[\frac{k_N}{k_S}\right]^{q-1}\left[(q+1)+q\left[\frac{\epsilon_N^T}{\epsilon_S^T}\right] - (q+1)\left[\frac{R_N}{R}\right]^{2q+1}\left[1-\frac{\epsilon_N^T}{\epsilon_S^T}\right]\right] , \tag{56}$$

which, for a small coating thickness, become

$$D_q \sim (k_N/k_S)^{q-1} , \tag{57a}$$

$$E_q \sim (\epsilon_N^T/\epsilon_S^T)(k_N/k_S)^{q-1} . \tag{57b}$$

On the other hand,

$$\sigma_q \sim -q\mu_S/\mu_N , \tag{58a}$$

$$\rho_q \sim q , \tag{58b}$$

$$\tau_q \sim (q+1)\frac{q+(q+1)(\mu_S/\mu_N)-q(R_N/R)^{2q+1}(1-\mu_S/\mu_N)}{q+(q+1)[(\mu_S/\mu_N)+(R_N/R)^{2q+1}(1-\mu_S/\mu_N)]} , \tag{58c}$$

$$\kappa_q \sim -(q+1)\left[\frac{\epsilon_M}{\epsilon_S^T}\right]\frac{(q+1)+q(\epsilon_N^T/\epsilon_S^T)+q(R_N/R)^{2q+1}(1-\epsilon_N^T/\epsilon_S^T)}{(q+1)+q(\epsilon_N^T/\epsilon_S^T)-(q+1)(R_N/R)^{2q+1}(1-\epsilon_N^T/\epsilon_S^T)} . \tag{58d}$$

In the limit of small shell thickness, τ_q and κ_q reduce to

$$\tau_q \sim q+1 , \tag{59a}$$

$$\kappa_q \sim -(q+1)\epsilon_M/\epsilon_S^T . \tag{59b}$$

Therefore, in this limit the coating plays a negligible role, and the resonances are those of a pure nucleus, i.e., from (45), and (58) and (59), one has

$$-q\mu_S/\mu_M = (q+1)\mu_S/\mu_N , \tag{60a}$$

$$q = -(q+1)\epsilon_M/\epsilon_N^T . \tag{60b}$$

One easily observes that the *latter* relation reduces to the Frölich condition *when $q=1$.*

For a *finite* thickness one finds

$$\mu_N\frac{q+(q+1)[(\mu_S/\mu_N)+(R_N/R)^{2q+1}(1-\mu_S/\mu_N)]}{(q+1)+q[(\mu_N/\mu_S)+(R_N/R)^{2q+1}(1-\mu_N/\mu_S)]} = -\frac{q+1}{q}\mu_M , \tag{61}$$

$$\epsilon_N^T\frac{q+(q+1)[(\epsilon_S^T/\epsilon_N^T)+(R_N/R)^{2q+1}(1-\epsilon_S^T/\epsilon_N^T)]}{(q+1)+q[(\epsilon_N^T/\epsilon_S^T)+(R_N/R)^{2q+1}(1-\epsilon_N^T/\epsilon_S^T)]} = -\frac{q+1}{q}\epsilon_M , \tag{62}$$

which can be explicitly rewritten *in the case $q=1$;* the left-hand side of Eq. (62) is then seen to be *identical* to the Van de Hulst expression (48) for ϵ_{cS}. These expressions thus generalize to, for all polar orders, well-known equivalent formulas for homogeneous spheres. In order to observe the first correction term to (60) it is easy to take the small-thickness limit in (61) and (62), i.e., for

$$Q^3 \equiv 1-\delta \simeq 1-3t/R , \tag{63}$$

one finds

$$\mu_N = -2\mu_M\frac{3-\delta(1-\mu_N/\mu_S)}{3-2\delta(1-\mu_S/\mu_N)} , \tag{64}$$

$$\epsilon_N = -2\epsilon_M \frac{3-\delta(1-\epsilon_N^T/\epsilon_S^T)}{3-2\delta(1-\epsilon_S^T/\epsilon_N^T)} \ . \tag{65}$$

We wish to recall that the above formulas are valid in the plasmonless limit [due to (55) and (56)] which is equivalent here to $\omega \ll \omega_p$.

C. Hollow sphere (in vacuum)

A particular case of technical interest is that of a dielectric bubble.[18] Although it would be more realistic to consider it suspended in a polar matrix (e.g., water), let us observe the interest of the previous formulas when $\epsilon_N = \epsilon_M = 1$. The resonances are found at

$$\frac{(\epsilon_S-1)^2}{(\epsilon_S+2)(2\epsilon_S+1)} = \frac{1}{2Q^3} \ , \tag{66}$$

while Clausius-Mosotti relation reads for an empty shell,

$$\frac{\epsilon_{cS}-1}{\epsilon_{cS}+2} = \frac{\delta}{g\epsilon_S}(1+2\epsilon_S)(\epsilon_S-1) \tag{67}$$

in the small-thickness limit.

The solution of Eq. (66) indicates that resonances exist for $\epsilon_S = -a \pm [(a^2-1)]^{1/2}$, where $4a = (4Q^3+5)/(1-Q^3)$. If the dielectric constant is a single-valued function, there is thus a direct and single correspondence between ω and the shell thickness, while the right-hand side of (67) gives the polarizability of an empty shell.

V. LONG-WAVELENGTH LIMIT

When the size of the particles is sufficiently small, one can consider that the fields do not vary greatly either in the nucleus or the shell. One can use a long-wavelength approximation, which here corresponds to x_N, x_S, y_N, and $x \rightarrow 0$. One can either rewrite the system of linear equations for the unknown field coefficients starting from (40) and (41) or repeat the calculation, but starting instead from the expansion of the potentials in terms of spherical harmonics. This procedure is less tedious than the theory presented in Sec. II because of the decoupling between the electric and magnetic modes in such a limit.

In fact, the long-wavelength limit is similar to the plasmonless limit on one hand, because it is equivalent to the simplification arising from the $\omega < \omega_p$ approximation. One can therefore observe that all expressions are available (see above) in order to calculate absorption spectra in the long-wavelength limit.

Furthermore, if only the dipolar terms are included, the theory leads to formulas derived by others or to results readily obtained from the above sections. Notice, however, that even in the long-wavelength limit it is of interest to include multipolar effects, in particular, when one considers dense clusters. The retardation effects are automatically included in the interaction matrix elements, and are calculated as in I.

Although we have observed elsewhere[1-4] that the long-wavelength limit leads to quite erroneous values in some cases (typically, of course, when the size of the particles is large) we will illustrate our *general* theory from results obtained from the long-wavelength approximation. This implies that the radius of the particles is less than 500 Å, but this is often quite sufficient (see Refs. 15–18 for exceptions).

VII. NUMERICAL RESULTS

Owing to the long-wavelength limit, the nucleus dielectric function can be considered to be plasmonless. We could choose a realistic dielectric function from experimental data, but will only present results when

$$\epsilon_N^L = \epsilon_N^T = \epsilon_b - \omega_p^2/[\omega(\omega+i\gamma_N)] \tag{68}$$

in units of $\epsilon_M = 1$.

Furthermore, the dielectric shell will be characterized by

$$\epsilon_S = \epsilon_\infty + (\epsilon_0 - \epsilon_\infty)/\{1-\omega^2/[\omega_T(\omega+i\gamma_S)]\} \tag{69}$$

in the usual notation.

In clusters we expect a large number of modes to appear (as in Refs. 28 and 29). The spectrum shape depends on the variation of several parameters: In addition to the characteristic parameters entering the dielectric function expressions, each particle radius, each layer thickness, and the particle separation can be modified. In general, even for the "simple" binary cluster, five parameters can be independently varied (four in the long-wavelength limit). Therefore, either cluster parameters and dielectric functions are selected to reproduce known experimental results, or an arbitrary selection of parameter variation is made, where we expect that sufficient information can be gained for further comparison with experimental data; analogy, intuition, and extrapolation are useful methods to be followed then. Notice that in the Appendix we present a brief discussion of the case in which a metallic shell covers a dielectric nucleus.

A. Single-particle spectrum

It is of interest to first recall the position of particle resonances, and thereby introduce notations. Equation (48) can be rewritten

$$\epsilon_{cS} = \epsilon_S(1+2Q^3 Z_N/Z_D)/(1-Q^3 Z_N/Z_D) \ , \tag{70}$$

where $Z_N = \epsilon_N - \epsilon_S$ and $Z_D = \epsilon_N + 2\epsilon_S$. Obviously, the numerator of the fraction in the above equation is larger than the denominator if $Z_N > 0$, i.e., if ϵ_N is greater than ϵ_S. Owing to the form of these dielectric functions, the positivity of Z_N is always satisfied, except for a frequency region between ω_T and the particular frequency at which

$\epsilon_{cS}=\epsilon_S=\epsilon_N$. The behavior of ϵ_{cS} can be easily obtained therefrom: (i) The zeroes of ϵ_{cS} occur at $\epsilon_S=0$, i.e., at ω_L, and when $Z_D+2Q^3Z_N=0$. (ii) The singularities of ϵ_{cS} occur at ω_T and for $Z_D=Q^3Z_N$. These (six) frequencies are called $\omega_i (i=1,\dots,6)$ and are ordered such that $\omega_1<\omega_2<\cdots<\omega_6$. A sketch of ϵ_{cS} is given in Fig. 1 with the appropriate definition of each ω_i.

One *a posteriori* observes that *three* solutions exist for the equation $\epsilon_{cS}+2\epsilon_M=0$. They are called ω_{SH}, ω_{SD}, and ω_{Sp} in increasing order. The notations are obvious: These are resonance frequencies due to the heterogeneous, dielectric, or metallic character of the particle, respectively. Indeed,

$$(\omega_{Sp}^*)^2\equiv\omega_{Sp}^2/\omega_p^2\simeq\tfrac{1}{3}\ , \tag{71a}$$

$$(\omega_{SD}^*)^2\equiv\omega_{SD}^2/\omega_p^2\simeq(\epsilon_0+2)/(\epsilon_\infty+2)\ . \tag{71b}$$

There is no such simple approximate value for ω_{SH}, but since ω_{SH} is below ω_T, one may take the limits $\omega_p^2\gg\omega_T^2-\omega_{SH}^2$ and $\epsilon_0\gg\epsilon_\infty$ and find $(\omega_T^*\equiv\omega_T/\omega_p)$

$$(\omega_{SH}^*)^2\equiv(\omega_{SH}^*)^2/(\omega_T^*)^2=\left[1+2\epsilon_0\left[\frac{1-2Q^3}{1+2Q^3}\right](\omega_T^*)^2\right]^{-1}\ . \tag{71c}$$

The validity of these approximations (71) is compared to exact values for a particular Q^3 value in Table I. One may finally obtain the range of "interesting regions" from the following observations: (i) $\omega_p\gg\omega_L>\omega_T$; (ii) $\omega_3-\omega_1<\omega_L-\omega_T$. Therefore, cluster spectra have to only be displayed between the following frequency bounds: (ω_1,ω_2), $(\omega_3\equiv\omega_T,\omega_4\equiv\omega_L)$, and (ω_5,ω_6). In absence of damping effects [$\gamma=0$ in (68) and (69)] the remaining frequencies are part of "spectral gaps."

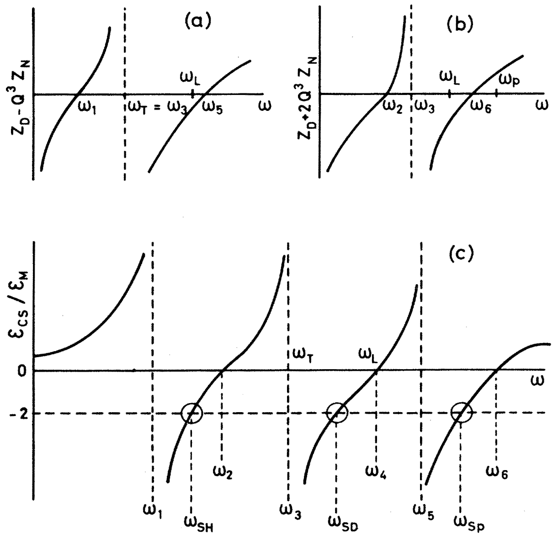

FIG. 1. Variation with frequency ω of the dielectric function ϵ_{cS} of an heterogeneous particle made of a metallic nucleus (N) and of a dielectric shell (S) in a vacuum matrix. Curve (c) is obtained by finding the zeros of $Z_D-Q^3Z_N$ [curve (a)] and those of $Z_D+2Q^3Z_N$ [curve (b)], the latter ones corresponding to singularities of ϵ_{cS}. $Z_D=\epsilon_N+2\epsilon_S$; $Z_N=\epsilon_N-\epsilon_S$. The frequencies ω_i ($i=1$ to 6) are thus easily defined. The spectrum of an isolated heterogeneous particle contains three peaks at ω_{SH}, ω_{SD}, and ω_{Sp}. The frequency scale is arbitrary.

TABLE I. Position of characteristic frequencies $\omega_i^*=\omega_i/\omega_p$ and of an isolated heterogeneous-sphere surface modes from Eq. (71) and from Van de Hulst (long-wavelength) theory. The particle is a metallic sphere, with plasmon frequency ω_p, surrounded by a dielectric shell with dielectric function parameters ϵ_0 and ϵ_∞. The metallic core is 60% of the total particle volume. ($\epsilon_0=9{,}8$; $\epsilon_\infty=2.95$; $Q^3=0.6$).

i	ω_i^*	Exact	Eq. (71)
1	0.108	$\omega_{SH}^*=0.187$	$\omega_{SH}^*=0.2075$
2	0.190		
3	0.200	$\omega_{SD}^*=0.345$	$\omega_{SD}^*=0.3087$
4	0.3645		
5	0.4075	$\omega_{Sp}^*=0.532$	$\omega_{Sp}^*=0.577$
6	0.732		

At this numerical stage, a choice of the core, coating, and matrix nature is in order; we have taken material characteristics to be those of sodium, rhodamine B, and vacuum, respectively. Table II gives the relevant parameter values. Table III lists all the characteristic frequencies for different layer thicknesses.

The above results have to be contrasted here with those of Ref. 26, where only one spectral line (corresponding to ω_{SD}) was found. This is due to the approximate dielectric function chosen by Ruppin; he chose $\epsilon_N=\infty$ for the metallic core.

B. Binary clusters

In order to display relevant information on the absorption spectrum of small clusters, or of a powder, either the absorption coefficient defined in terms of the imaginary part of the averaged complex susceptibility, or the total absorbed power can be calculated.[1]

The absorption coefficient is the weighted sum of each individual sphere absorption coefficient. Since the denominator of Eq. (48) and the left-hand side of Eq. (62) vanish at more than one frequency, in order to present the frequency dependence, we cannot write an expression as trivial as Eq. (35) of Ref. 1. Therefore, we prefer to recall that the total power absorbed by a sphere B of volume v_B is

TABLE II. Parameter values for the metallic core surrounded by a dielectric shell for heterogeneous particles hereby considered.

Metallic core	Dielectric shell	Vacuum matrix
$\epsilon_b=1.0$	$\epsilon_0=1.0408$	$\epsilon_0=1.0$
$\gamma=10^{-5}$	$\epsilon_\infty=1.0$	$\epsilon_\infty=1.0$
$\omega_p=1.0$	$\omega_T=0.380\,85\omega_p$	$\omega_T=0.0$
	$\gamma=2.7203\times10^{-2}$	$\gamma=0.0$
	$\omega_L=0.388\,54\omega_p$	

TABLE III. Values of bound frequencies and of surface-mode frequencies for a single heterogeneous particle of radius R in a vacuum matrix for parameter values given in Table II: the core is metallic and the dielectric shell has a thickness t. $Q=1-t/R$. All reduced frequency values are multiplied by a factor 10^5.

t	R	Q	Q^3	ω_1^*	ω_{SH}^*	ω_2^*	ω_{SD}^*	ω_5^*	ω_{Sp}^*	ω_6^*
0	1.0	1.0	1.0			38085		38854	57735	10^5
0.1	1.0	0.909	0.7513	27711	38042	38058	38669	39570	57887	91440
0.2	1.2	0.833	0.5787	34368	37995	38030	38560	41527	57991	84924
0.5	1.5	0.667	0.2963	37218	37877	37949	38426	49561	58157	73121
1.0	2.0	0.500	0.1250	37566	37779	37847	38372	54753	58256	69956
2.0	3.0	0.333	0.0373	37665	37723	37754	38351	57288	58306	60360

$$W(B,\omega)=\epsilon_{cS}^{B}(\omega)\int_{v_B} d\vec{r}_B\,|\vec{E}(B,\omega)|^2/(\epsilon_M E_0)^2\,, \quad (72)$$

and to sum each term in order to obtain the total absorbed power for N spheres occupying a volume v,

$$W(\omega)=(1/v)\sum_{B=1}^{N} W(B,\omega)\,. \quad (73)$$

The active power $\mathrm{Im}\,W\equiv W''$, and the reactive power $W'\equiv\mathrm{Re}W$ can be related to usual optical properties. The reactive power being a linear function of the real part of the dielectric constant $\epsilon_{cS}(\omega)$ can be related to the imaginary part through Kramers-Kronig relations.

The reactive power (in fact, its logarithm) is thus displayed below. It presents the qualitative features to be observed experimentally.

Only linear clusters have been investigated. It is known from the theory of Clippe *et al.*[28] and applications[23,24,29,36,37] that such chainlike systems give a sufficiently good approximation to several powder systems. This analysis does not consider the actual presence of globules in a powder.

Also, note that only the variations of the resonance modes as a function of the various parameters are usually presented. Here we show the *whole spectrum* behavior which necessitates the solution of the matrix equation derived in Sec. II, since the (square of the field expansion) coefficients themselves are necessary in order to calculate $W(\omega)$. *Mutatis mutandis,* such a lengthy expression has been given in I [Eq. (40)]. Furthermore, only two angles of light incidence are considered: The k vector is either parallel or perpendicular to the chain axis. Intermediary cases are superpositions of such spectra with the appropriate $(\cos^2\theta,\sin^2\theta)$ weight, where θ is the angle between the k vector of the light and the cluster symmetry axis (see, e.g., Fig. 2).

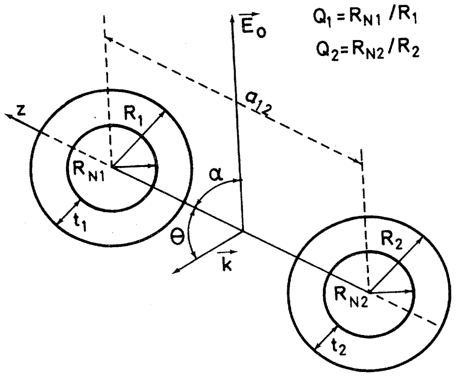

FIG. 2. Definition of geometrical parameters for a cluster of two spherical heterogeneous particles in an electromagnetic field of wave vector $\vec{k}$.

We have selected to examine binary clusters here, looking for limiting cases that are likely to encompass many situations. The binary cluster examined consists of a homogeneous particle (for instance, 1) of fixed radius R_1, a second particle (for instance, 2) of radius R_2, and varying layer thickness t_2. In Figs. 3(a)—3(i) we show the variation of $\ln(\mathrm{Re}\,W)$ as a function of $\omega^*\equiv\omega/\omega_p$. The angle α of the electric field $\vec{E}_0$ (of the incident light), with the z axis on which the cluster is aligned, is chosen to be 0 or $\pi/2$.

It is indeed known that in the long-wavelength limit the absorption effects may be simply discussed for such cases only, irrespective of the light incidence and position of the $\vec{H}_0$ vector (hence of the $\vec{k}$ vector).[38] The shadow effects which appear when the incident wave vector is parallel to the center to center axis, and both $\vec{E}_0$ and $\vec{H}_0$ are perpendicular to this axis, are not discussed here. One might just admit that we take $\vec{k}$ perpendicular to both z and $\vec{E}_0$. An extra (small) peak at lower energy would occur otherwise when the spheres have the same radius, and only then. Owing to the complication of carrying such an extra particular case, we have left it out of our computer program here.

We show effects which result from only taking into account terms to the dipolar [Figs. 3(a)—3(c)], quadrupolar [Figs. 3(d)—3(f)], and octupolar [Figs. 3(g)—3(i)] order in three cases, i.e., $R_1=1$ and $R_2=1.1$, 1.5, and 2.0, thus with $t_2=0.1$, 0.5, and 1.0, respectively. In each case the particles are supposed to be in contact such that $a_{12}=R_1+R_2$. In this case indeed, the high-order polar terms are of importance, as shown elsewhere in the case of homogeneous spheres.[1–5,39,40] The logarithmic scale for W' renders the spectrum to be slightly awkward at first sight. Nevertheless, in the dipolar approximation one easily recognizes the three regions mentioned above, corre-

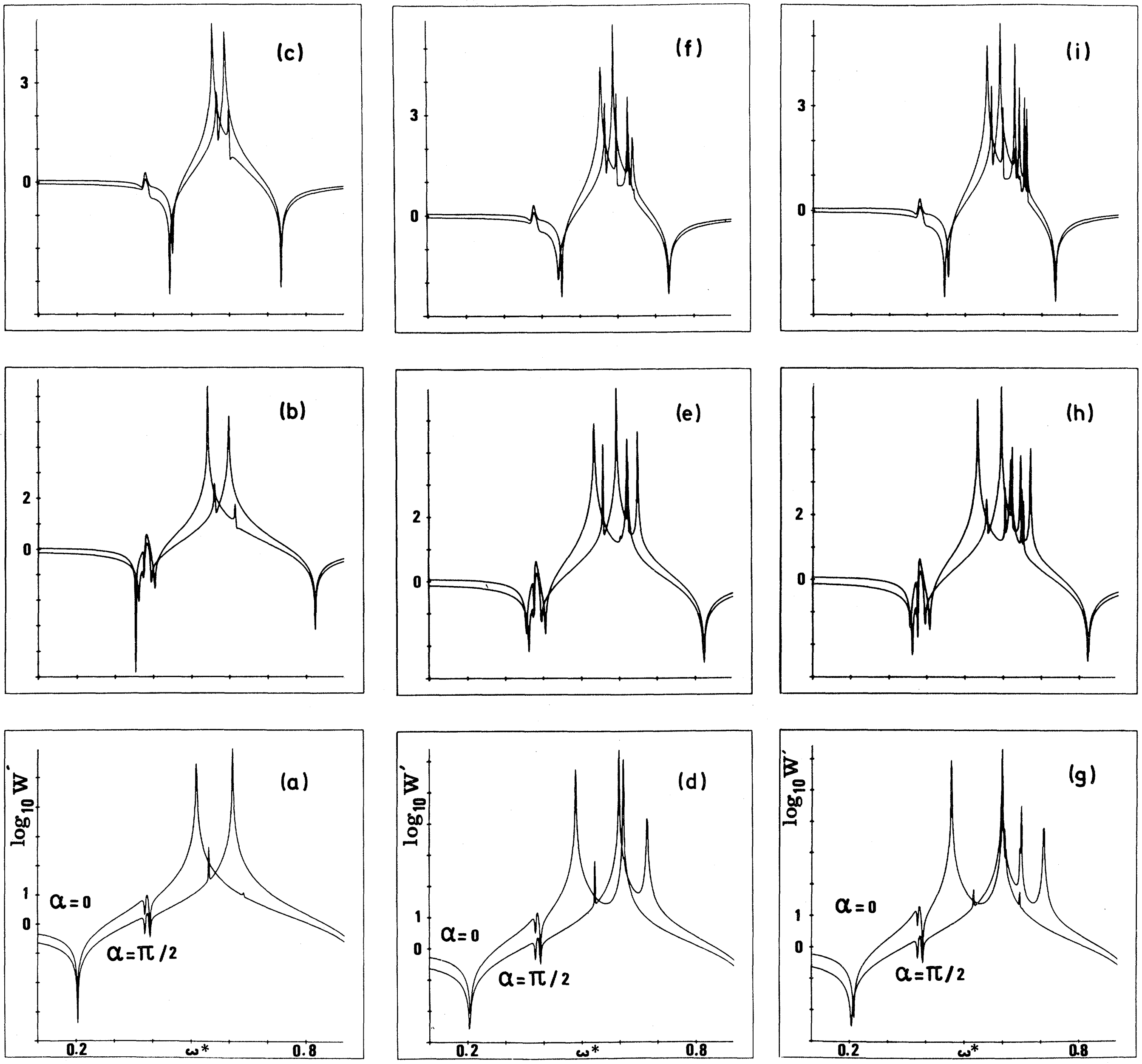

FIG. 3. Variation of the reactive power of a binary cluster of two touching metallic spheres, one of them being coated by a dielectric material, for different values of the layer thickness t, and hence of the particle radius R, as a function of reduced frequency $\omega^* = \omega/\omega_p$, where ω_p is the plasmon frequency. The curves are obtained by limiting the interactions to the (a)—(c) dipolar, (d)—(f) quadrupolar, and (g)—(i) octupolar terms, and by taking the long-wavelength limit. Two angles of light incidence are considered; $t=0.1$ in (a), (d), (g); $t=0.5$ in (b), (e), (h); $t=1.0$ in (c), (f), (i).

sponding to three ensembles of surface modes. As in Ref. 28, each independent-sphere surface mode is split by the mutual interaction. It is interesting to note that the "plasmon surface modes" lead to the largest amplitude, while the ω_{SH}-like modes, shifted toward low ω values, are relatively weak. The relative amplitudes depend in the same way on the $\vec{E}_0$ field incidence angle as in the case of homogeneous spheres. The larger amplitude occurs at higher frequency when $\vec{E}_0$ is perpendicular to the line joining the sphere centers.

When the coating thickness increases, the size of the absorption regions is much modified: Region III markedly shrinks and becomes quite narrow (here, betwen 0.45 and 0.72) when the layer thickness is equal to the core radius. If the coating thickness would increase further, one would have the situation of a single homogeneous metallic parti-

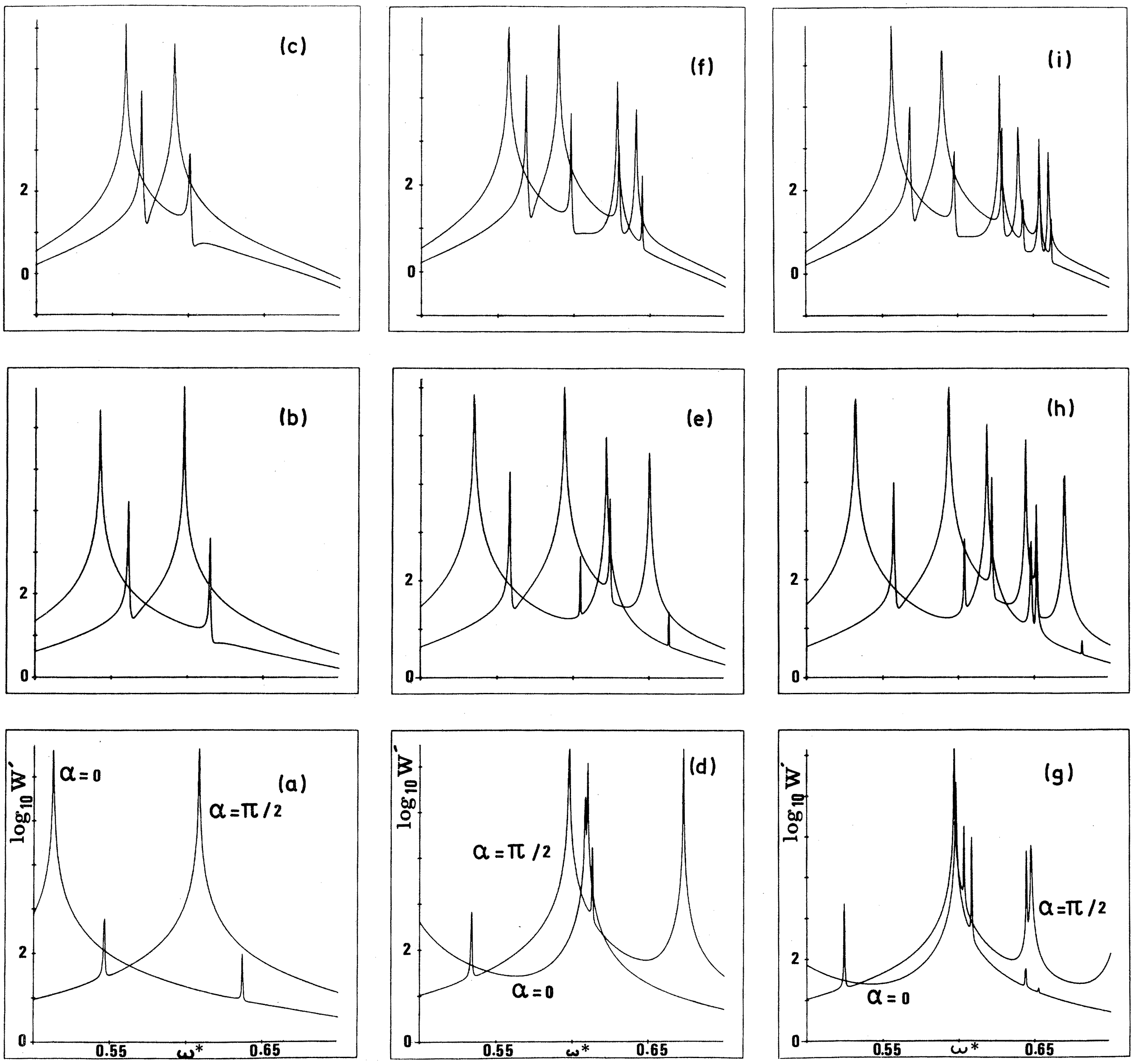

FIG. 4. Same as for Fig. 3, but for the region between ω_5^* and ω_6^* that encompasses the plasmon surface modes near ω_{Sp}^*.

cle in the presence of a dielectric surface (containing an "irrelevant" deep inclusion). The single-resonant mode would fall near $\omega^* = 0.59$. Region II shrinks on the other hand, but contains much structure, when the layer thickness increases, but remains smaller than the core radius ($t_2 < R_2/2$). In such a case, the dielectric layer modes are quite noticeable. When the layer thickness becomes larger, however, its influence takes a different nature: The coating volume indeed becomes larger than the core. Thus, the dielectric (dye) "surface modes," which originate in the coating material, tend to disappear as if the layer had already reached a bulky appearance. Finally, region I always grows toward higher ω^* values and, as we have just seen, incorporates region II because the heterogeneity of the particle appears less important. Region III disappears when $R_1 = t_2 = R_2/2$. Only a small peak (near $\omega^* = 0.35$) is still reminiscent of the heterogeneous nature of particle 2. For all these cases, region III has been enlarged in Figs. 4(a)–4(c).

Next, we observe the effects of higher-order polar terms. The number of resonant modes increases as in Figs. 3(d)–3(i). In region III, the four dipolar modes split into eight when quadrupolar terms are included [see also Figs. 4(d)–4(f)] and into 12 modes, as expected of course, when octupolar terms are taken into account [Figs. 4(g)–4(i)]. For small layer thicknesses, several of these modes are weakly absorbing, and thus appear as shoulders only on the main peaks.

The clearest mode-distribution figure is again that for an intermediate thickness value $t_2=0.5$. In such a case, the core modes are similar to those discussed in Ref. 28.

It is interesting to note that regions I and II do not *apparently* contain more modes when high-order polar terms are included [see Figs. 3(e) and 3(h), for example]. We have seen in Ref. 1, that the inclusion of such terms for binary clusters of ionic spheres did not lead to strong values of the absorption spectrum, but to very small shoulders. As noticed later,[4] the structure is masked by the (large) dipolar peaks, and the multiplicity of peaks is likely unobservable then. Furthermore, we may point out that we have checked the effect of smaller or larger damping factors than those used here (Table II). There is no great change in the precision of the data if the core damping constant $\gamma_N=10^{-5}$ is replaced by $\gamma_N=10^{-2}$. On the other hand, to take $\gamma=0$ would lead to unrealistic δ functions for the power spectrum. Therefore, we have not shown enlargements of regions I and II, nor do we show any spectrum with values other than those given in Table II. We do not claim, however, that to examine these spectral regions is uninteresting. On the contrary, it might be useful to do so in order to understand the nature of coating layers. However, fine-resolution experiments would have to be done then.

It is obviously apparent that the narrowness of regions I and II is due to the small value of $\omega_L-\omega_T$ (and of ω_L and ω_T with respect to the plasmon frequency ω_p). The structure in these regions might be made more apparent if the core and layer dielectric functions were more similar.

C. Separation effects

High-order polar terms are known to be more relevant when particles are in close contact. On the other hand, when particles are greatly separated, they respond independently to the incident field. A great amount of work has been done in such a case (see also Sec. VII A). Therefore, we may expect that separation effects can be simply discussed from previous work.[1,5]

The number of resonant modes is, of course, unchanged with respect to the touching-sphere case. The multiple-peak structure is conserved for a rather large separation a_{ij}; typically, for a_{ij} greater than 5 times the largest radius, the mutual interaction is negligible, and the particles can be said to be independent: This is due to the fall of the interaction $V_{11}^{(m)}$ which decreases as $1/(ka_{ij})^3$. Notice that such a value gives an idea of how dispersed a system must be in order to be considered as diluted, i.e., the concentration must be lower then $1/2^5$, viz., 3%. Interpretations of experimental results on heterogeneous particles with a higher concentration must be taken with caution. Obviously, powder systems must include some analysis based on high-order polar effects and statistics of clusters. This is outside the scope of the present publication, however. Also, note that at higher separation the information contained in the polarization (or the angle α) is then lost due to the independent-particle response.

D. Other effects

If a matrix other than vacuum is chosen to support the clusters, it is expected that due to the larger value of ϵ_N, the modes will pile up at lower frequencies. This was checked. It might be of interest to consider the case of a matrix with a frequency-dependent dielectric function as for colloidal suspensions in water. An interesting complex case would be that of magnetic cores.[41] We intend to pursue some work in such a direction. Of course, our theory must then be generalized in order to take into account that the k vector in the matrix has an imaginary part. The geometry of the incident wave would have to be modified as well.

Finally, it has been noticed in the literature that the absorption of small metal-particle composites can be of several orders of magnitude above theoretical calculations. It is likely that such a remark holds true for isolated aggregates. It has been proposed that size-distribution effects[42,43] greatly influence the absorption coefficient value. Chylek and Srivastava have considered the effect of magnetic dipole absorption for composites.[44] Such effects are of course included in our theory. We have indeed noticed that the extinction cross section (obtained from the ratio of the power W'' to the power flow per unit area of the incident wave) contains such effects,[5] or that the main peak of the absorption spectrum of small clusters of homogeneous particles grows in value when high-order polar terms are included.[4] It is expected that such effects remain as noticeable in the case of heterogeneous particle clusters.

In conclusion, although we have examined the most simple generalizatoin of a binary cluster, i.e., with only

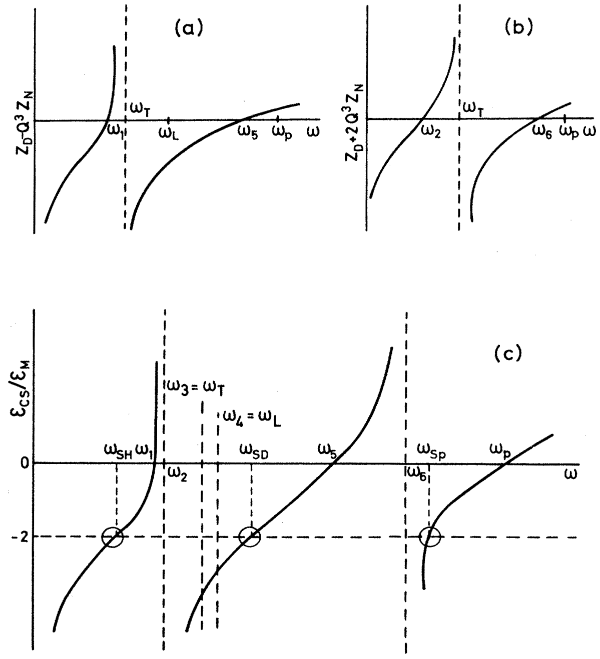

FIG. 5. Same as Fig. 1, but when the heterogeneous particle is made of a dielectric core surrounded by a metallic shell.

TABLE IV. Same as Table III but for a dielectric core and a metallic shell.

t	R	Q	Q^3	ω^*_{SH}	ω^*_1	ω^*_2	ω^*_{SD}	ω^*_5	ω^*_6	ω^*_{Sp}
0.0	1.0	1.0	1.0			38 085	37 343	38 854		
0.1	1.1	0.909	0.7513	23 994	35 806	38 073	38 455	43 309	95 796	97 035
0.2	1.2	0.833	0.5787	31 785	37 519	38 062	38 732	53 796	92 767	94 656
0.5	1.5	0.667	0.2963	37 670	37 903	38 042	44 504	68 823	87 587	89 836
1.0	2.0	0.500	0.1250	37 942	37 978	38 027	51 545	76 590	84 291	85 870
2.0	3.0	0.333	0.037	37 997	38 004	38 018	55 741	80 294	82 549	83 183
							57 735			10^5

one heterogeneous particle, we expect to have shown that we have extended theoretical work on optical (infrared) properties of small particles in an aggregate state, and have included all relevant parameter effects in order to consider cases where heterogeneous particles are found. We hope that this can be useful in experimental work on specific cases.

APPENDIX

In this appendix we briefly discuss the case of particles with a dielectric core and a surrounding metallic layer. Although this might appear at first unusual, it is a better representation of metallic particles in fact: Owing to the chemical production process, metallic particles are in fact grown on a dielectric seed. Thus, we may examine the representative case as that of Fig. 2, remembering that a large thickness t is a realistic limit.

The single-particle spectrum is slightly different from that reported in Sec. VII since there is an interchange between ϵ_S and ϵ_N. Therefore, the variation of ϵ_{cS} with ω is that sketched in Fig. 5. The interesting spectral limits are now $(0,\omega_1)$, (ω_2,ω_5), and $(\omega_6,1)$. Notice that a sharp line is further expected at ω_T, while the position of ω_{SD} with respect to ω_T and ω_L greatly depends on parameter values. A table (Table IV) of the characteristic frequencies is given for the symmetric case of that studied in Sec. VII, even though we realize that sodium grown on rhodamine B is most likely a very particular case!

Concerning the spectrum of clusters of metallic particles with a dielectric core, the same discussion as that made in Sec. VII may follow. Let us note that ω^*_{SH} is very close to ω^*_1, since region I is very narrow. In region II, which becomes rather large with increasing metallic content, ω^*_{SD} almost reaches the value $\frac{1}{3}$ when $R \simeq 3t/2$. Region III obviously shrinks with increasing t. Therefore, for such particles in clusters, the interesting region to examine is region II. *Mutatis mutandis* (in particular the frequency bounds), the spectrum in such a region II is similar to that shown in Fig. 4.

---

[*] Present address: MMCT, rue des Français 216, B-4300 Ans, Belgium.

[†] From whom reprints may be requested.

[1] J. M. Gérardy and M. Ausloos, Phys. Rev. B 22, 4950 (1980).

[2] M. Ausloos, P. Clippe, and J. M. Gérardy, *Le vide, les couches minces,* Suppl. 21, 201, 758 (1980).

[3] J. M. Gérardy and M. Ausloos, in *Recent Developments in Condensed Matter Physics,* edited by J. T. Devreese, L. Lemmens, V. Van Doren, and J. Van Royen (Plenum, New York, 1981), Vol. 3, p. 347.

[4] J. M. Gérardy and M. Ausloos, Surf. Sci. 106, 319 (1981).

[5] J. M. Gérardy and M. Ausloos, Phys. Rev. B 25, 4204 (1982).

[6] R. Ruppin, Phys. Rev. B 11, 2871 (1975).

[7] Proceedings of the Conference on Surface Properties and Surface States of Electronic Materials, Rolla 1972 [Surf. Sci. 34, 1 (1973)].

[8] Proceedings of the 1st International Conference on the Small Particles and Inorganic Clusters, Lyon, 1976 [J. Phys. (Paris) Colloq. 38, C2-1 (1977)].

[9] *Electrical Transport and Optical Properties of Inhomogeneous Media (Ohio State University, 1977),* Proceedings of the First Conference on the Electrical Transport and Optical Properties of Inhomogeneous Media, edited by J. C. Garland and D. B. Tanner (AIP, New York, 1978), pp. 1—98, 193—358.

[10] Proceedings of the 2nd International Conference on the Small Particles and Inorganic Clusters, Lausanne 1980 [Surf. Sci. 106, 1 (1981)].

[11] J. A. A. J. Perenboom, P. Wyder, and F. Meier, Phys. Rep. 78, 173 (1981).

[12] A. Güttler, Ann. Phys. (Leipzig) 11, 65 (1952).

[13] A. L. Aden and M. Kerker, J. Appl. Phys. 22, 1242 (1951).

[14] D. S. Wang and M. Kerker, Phys. Rev. B 25, 2433 (1982), where an interesting ensemble of references can be found.

[15] M. Kerker, J. Coll. Interface Sci. 58, 100 (1977).

[16] C. F. Bohren, J. Chem. Phys. 62, 1566 (1975).

[17] D. J. Gordon and G. Holzwarth, Proc. Natl. Acad. Sci. USA 68, 2365 (1971).

[18] P. Latimer and F. Wamble, Appl. Opt. 21, 2447 (1982), and references therein.

[19] M. E. Milham, D. H. Anderson, and R. H. Frickel, Appl. Opt. 21, 2501 (1982).

[20] L. Blum and H. L. Frisch, J. Polym. Sci. 14, 1743 (1976).

[21] A. A. Lushnikov, V. V. Maksimenko, and A. J. Simonov, Solid State Commun. 20, 545 (1976); Z. Phys. B 27, 321 (1977).

[22] L. Genzel, T. P. Martin, and U. Kreibig, Z. Phys. B 21, 339 (1975).

[23] C. G. Granqvist and O. Hunderi, Z. Phys. B 30, 47 (1978).

[24] C. G. Granqvist, N. Calander, and O. Hunderi, Solid State Commun. 31, 249 (1979).

[25] T. P. Martin, Solid State Commun. 17, 139 (1975).

[26] R. Ruppin, Surf. Sci. 51, 140 (1975).

[27] J. H. Weaver, R. W. Alexander, L. Teng, R. A. Mann, and R. J. Bell, Phys. Status Solidi A 20, 321 (1973).

[28] P. Clippe, R. Evrard, and A. A. Lucas, Phys. Rev. B 14, 1715 (1976).

[29] M. Ausloos, P. Clippe, and A. A. Lucas, Phys. Rev. B 18, 7176 (1978).

[30] P. Clippe and M. Ausloos, Phys. Status Solidi B 110, 211 (1982).

[31] J. E. Sansonetti and J. K. Furdyna, J. Appl. Phys. 50, 2899 (1979).

[32] J. M. Gérardy and M. Ausloos, Phys. Rev. B 26, 4703 (1982).

[33] D. M. Wood and N. W. Ashcroft, Philos. Mag. 35, 269 (1977).

[34] P. Sheng, Phys. Rev. Lett. 45, 60 (1980).

[35] A. R. Melnyk and M. J. Harrison, Phys. Rev. B 2, 835 (1970).

[36] U. Kreibig, A. Althoff, and H. Pressman, in *Proceedings of the 2nd International Conference on the Small Particles and Inorganic Clusters,* Ref. 10, p. 308.

[37] P. O'Neill, A. Ignatiev, and C. Doland, in *Electrical Transport and Optical Properties of Inhomogeneous Media (Ohio State University, 1977),* Ref. 9, p. 288.

[38] J. M. Gérardy and M. Ausloos, Phys. Rev. B 27, 6446 (1983).

[39] F. Claro, Phys. Rev. B 25, 7875 (1982).

[40] R. Ruppin, Phys. Rev. B 26, 3440 (1982).

[41] J. C. Bacri and D. Salin, J. Phys. (Paris) Lett. 43, L771 (1982).

[42] P. Chylek, D. Boice, and R. G. Pinnick, Phys. Rev. B 27, 5107 (1983).

[43] J. M. Gérardy and M. Ausloos, Phys. Rev. B 26, 4703 (1982).

[44] P. Chylek and D. Srivastava, Phys. Rev. B 27, 5098 (1983).